Article

Current Biology

Kinesin-Binding Protein Controls Microtubule Dynamics and Cargo Trafficking by Regulating Kinesin Motor Activity

Graphical Abstract

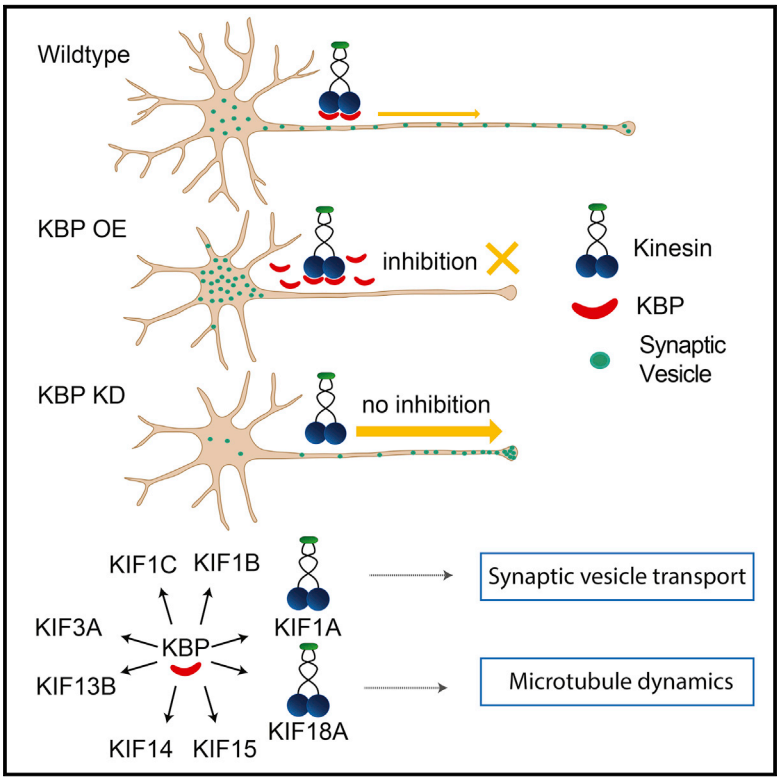

Highlights

- KBP binds to the motor domain of a subset of kinesin motor proteins
- KBP prevents kinesin motility by inhibiting microtubule binding
- KBP modulates neuronal cargo transport and microtubule dynamics
- Misregulation of KBP-controlled kinesins may contribute to GOSHS

Authors

Josta T. Kevenaar, Sarah Bianchi, Myrrhe van Spronsen, ..., Anna Ahkmanova, Michel O. Steinmetz, Casper C. Hoogenraad

Correspondence

c.hoogenraad@uu.nl

In Brief

Kinesin motors are a large family of related motor proteins that are essential for various microtubule-based processes during neuronal development and homeostasis. Kevenaar et al. found that kinesin-binding protein (KBP) is a specific kinesin inhibitor that modulates microtubule-based motility and depolymerizing activity of a subset of kinesins.

Kevenaar et al., 2016, Current Biology *26*, 849–861
April 4, 2016
http://dx.doi.org/10.1016/j.cub.2016.01.048

Current Biology
Article

Kinesin-Binding Protein Controls Microtubule Dynamics and Cargo Trafficking by Regulating Kinesin Motor Activity

Josta T. Kevenaar,[1,6] Sarah Bianchi,[2,6] Myrrhe van Spronsen,[1,3,6] Natacha Olieric,[2] Joanna Lipka,[1,4] Cátia P. Frias,[1] Marina Mikhaylova,[1,5] Martin Harterink,[1] Nanda Keijzer,[3] Phebe S. Wulf,[1,3] Manuel Hilbert,[2] Lukas C. Kapitein,[1,3] Esther de Graaff,[1,3] Anna Ahkmanova,[1] Michel O. Steinmetz,[2] and Casper C. Hoogenraad[1,3,*]
[1]Cell Biology, Department of Biology, Faculty of Science, Utrecht University, 3584 Utrecht, the Netherlands
[2]Laboratory of Biomolecular Research, Department of Biology and Chemistry, Paul Scherrer Institute, 5232 Villigen PSI, Switzerland
[3]Department of Neuroscience, Erasmus Medical Center, 3015 Rotterdam, the Netherlands
[4]International Institute of Molecular and Cell Biology, 02-1009 Warsaw, Poland
[5]RG Neuroplasticity, Leibniz-Institute for Neurobiology, 39118 Magdeburg, Germany
[6]Co-first author
*Correspondence: c.hoogenraad@uu.nl
http://dx.doi.org/10.1016/j.cub.2016.01.048

SUMMARY

Kinesin motor proteins play a fundamental role for normal neuronal development by controlling intracellular cargo transport and microtubule (MT) cytoskeleton organization. Regulating kinesin activity is important to ensure their proper functioning, and their misregulation often leads to severe human neurological disorders. Homozygous nonsense mutations in kinesin-binding protein (KBP)/KIAA1279 cause the neurological disorder Goldberg-Shprintzen syndrome (GOSHS), which is characterized by intellectual disability, microcephaly, and axonal neuropathy. Here, we show that KBP regulates kinesin activity by interacting with the motor domains of a specific subset of kinesins to prevent their association with the MT cytoskeleton. The KBP-interacting kinesins include cargo-transporting motors such as kinesin-3/KIF1A and MT-depolymerizing motor kinesin-8/KIF18A. We found that KBP blocks KIF1A/UNC-104-mediated synaptic vesicle transport in cultured hippocampal neurons and in *C. elegans* PVD sensory neurons. In contrast, depletion of KBP results in the accumulation of KIF1A motors and synaptic vesicles in the axonal growth cone. We also show that KBP regulates neuronal MT dynamics by controlling KIF18A activity. Our data suggest that KBP functions as a kinesin inhibitor that modulates MT-based cargo motility and depolymerizing activity of a subset of kinesin motors. We propose that misregulation of KBP-controlled kinesin motors may represent the underlying molecular mechanism that contributes to the neuropathological defects observed in GOSHS patients.

INTRODUCTION

Kinesin motors are a large family of related motor proteins that are essential for various microtubule (MT)-based processes during neuronal development. Kinesins drive vesicle transport, organize the localization of organelles, and control MT dynamics in both axons and dendrites [1–3]. Several mechanisms exists that control kinesin motor activity, both at the level of motor-cargo and motor-MT interactions [4, 5]. One important mechanism by which motor proteins are regulated includes the suppression of motor activity by autoinhibition, which has been best studied for kinesin-1 family members [6]. In the absence of cargo, inactive kinesin-1 exists in a folded conformation, allowing the tail domain to bind and inhibit its motor domain [7]. Cargo binding of the tail region subsequently relieves autoinhibition and enables MT-based motility [8, 9]. However, whether other kinesin inhibitory mechanisms exist is unknown.

Human genetics studies showed that homozygous nonsense mutations in the gene encoding kinesin-binding protein (KBP/KIAA1279) were linked to Goldberg-Shprintzen syndrome (GOSHS), a severe neurological disorder characterized by intellectual disability, polymicrogyria, microcephaly, and axonal neuropathy [10–12]. KBP was originally identified as a KIF1C-binding protein [13] and was found to be associated with other members of the kinesin family [14, 15]. Furthermore, KBP has been suggested to associate with the cytoskeleton [16, 17] and shown to be required for axonal outgrowth in zebrafish [18]. Interestingly, electron microscopy analysis of the KBP zebrafish mutants revealed MT defects and aberrant organelle accumulations in the axon [18]. However, the function of KBP and its putative role in regulating MT dynamics and cargo transport has remained unresolved.

In this study, we found that KBP binds to the motor domain of a specific set of kinesin family members and regulates kinesin activity by preventing the association of the kinesin with MTs. Our findings suggest that KBP functions as a specific kinesin inhibitor that modulates MT-based motility and depolymerizing activity of distinct kinesin motors. Inhibition of kinesin activity by KBP provides a novel control mechanism for kinesin motor protein function.

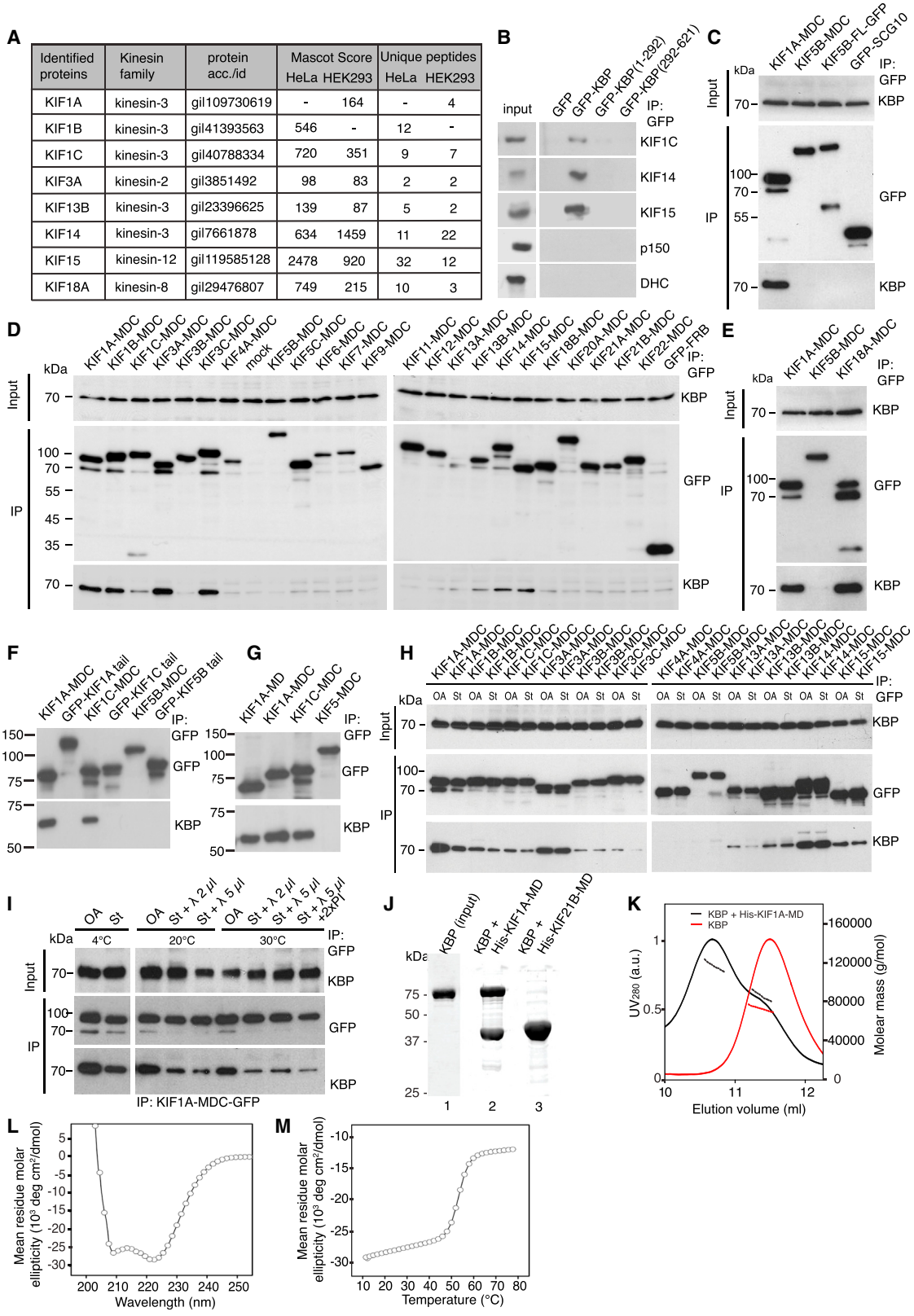

Identified proteins	Kinesin family	protein acc./id	Mascot Score HeLa	Mascot Score HEK293	Unique peptides HeLa	Unique peptides HEK293
KIF1A	kinesin-3	gil109730619	-	164	-	4
KIF1B	kinesin-3	gil41393563	546	-	12	-
KIF1C	kinesin-3	gil40788334	720	351	9	7
KIF3A	kinesin-2	gil3851492	98	83	2	2
KIF13B	kinesin-3	gil23396625	139	87	5	2
KIF14	kinesin-3	gil7661878	634	1459	11	22
KIF15	kinesin-12	gil119585128	2478	920	32	12
KIF18A	kinesin-8	gil29476807	749	215	10	3

Figure 1. KBP Binds to the Motor Domain of a Specific Subset of Kinesin Family Proteins

(A) Most prominent binding partners of bio-GFP-KBP in HeLa and HEK293 cells identified by mass spectrometry.

(B) Immunoprecipitations using GFP antibodies from extracts of HEK293 cells transfected with the indicated constructs and probed with the indicated antibodies.

(legend continued on next page)

RESULTS

KBP Binds to the Motor Domain of a Specific Subset of Kinesin Motor Proteins

KBP was originally identified in a yeast two-hybrid screen as a KIF1C-binding protein [13] and was found to be associated with other members of the kinesin-3 family [14, 15]. To identify additional KBP-binding partners, we made use of pull-down assays combined with mass spectrometry using biotinylated and GFP-tagged KBP (bio-GFP-KBP) in HEK293 or HeLa cells. Several types of kinesin motors were identified in this analysis: the kinesin-2 motor KIF3A; members of the kinesin-3 family, including KIF1A, KIF1B, KIF1C, KIF13B, and KIF14; kinesin-8 motor KIF18A; and kinesin-12 motor KIF15 (Figure 1A). Other molecular motors, such as components of the dynein/dynactin motor complex or myosin proteins, kinesin-1 (KIF5/KHC), kinesin-4 (KIF21), kinesin-13 (KIF2/M-kinesins), and kinesin-14 (KIFC/C-kinesins), were not detected in the KBP pull-down experiments. To validate the mass spectrometry results and to further narrow down the kinesin-KBP interaction, we conducted pull-down and immunoprecipitation experiments using KBP-specific antibodies (Figures S1A and S1B). Using a panel of GFP-tagged kinesin proteins containing only the motor domain and the first coiled-coil region (MDC), we could confirm that endogenous KBP binds to the same subset of kinesins that were identified by mass spectrometry (Figures 1D and 1E). Consistent with the mass spectrometry results, several other kinesin family members, including the kinesin-1 motor KIF5B and the kinesin-4 motor KIF21B, or components of the dynein motor did not pull-down endogenous KBP (Figures 1C, 1D, and S1D), indicating that KBP binds to a specific subset of kinesin motor proteins. Using similar pull-down and immunoprecipitation assays, we could not detect the previously described association between the stathmin-like protein SCG10 and KBP [16] (Figures 1C and S1D).

To corroborate that KBP binds specifically to the motor domain as suggested by our pull-down experiments (Figures 1D and 1E), we performed additional immunoprecipitation experiments with constructs containing either the MDC domain or the whole stalk/tail region (tail) of the kinesin-3 family members KIF1A and KIF1C (Figure 1F). In agreement with the previous experiments (Figures 1A and 1D), KBP did not interact with any of the kinesin tail constructs but associated with the motor domains of KIF1A and KIF1C, whereas it showed no interaction with full-length KIF5B or its motor domain (Figures 1C, 1F, and S1D). Furthermore, KBP is also able to interact with a single motor domain of KIF1A, without the coiled-coil region (MD; Figure 1G). By expressing truncated versions of KBP, we tried to map the minimal kinesin-binding region of KBP (Figure S1A). Whereas none of the N-terminal (amino acids [aa] 1–292) and C-terminal (aa 292–621) fragments of KBP were able to interact with any of the kinesin constructs, full-length KBP (aa 1–621) bound to endogenous KIF1C, KIF14, and KIF15 (Figures 1B and S1C).

In Vitro Characterization of KBP and Its Interaction with the Motor Domain of KIF1A

To further characterize the function of KBP in vitro, we used affinity-purified, recombinant KBP from bacteria (Figure 1J, lane 1). We first conducted multiangle light scattering (MALS) experiments to assess the oligomerization state of KBP in solution and obtained a molecular mass of 69.7 kDa (Figure 1K, red line), which is consistent with the molecular mass of monomeric KBP (71.9 kDa). Circular dichroism (CD) spectroscopy measurements of KBP revealed a far-UV spectrum characteristic of proteins with substantial α-helical content (Figure 1L). The stability of KBP was assessed by a thermal unfolding profile recorded by CD at 222 nm (Figure 1M), which revealed a single sharp transition with a melting temperature, Tm, centered at 53°C. These findings are consistent with sequence analysis and structure predictions, which indicate that KBP exhibits an alpha-alpha superhelix type of fold formed by three tetratricopeptide-like repeats (TPR) (Figure S1A).

To study the interaction between KBP and kinesin in more detail, we used one of the best-studied kinesins, KIF1A, as our representative motor protein and tested whether KBP binds directly to the motor domain of KIF1A (KIF1A-MD). His-KIF1A-MD co-eluted in the presence of an excess of untagged KBP (Figure 1J, lane 2), thus demonstrating a direct interaction between KBP and the motor domain of KIF1A. In contrast, His-KIF21B-MD did not co-elute with KBP, indicating that the interaction is specific for KIF1A-MD (Figure 1J, lane 3). To assess the stoichiometry of the KBP/His-KIF1A-MD complex, we performed MALS experiments with the co-purified complex and obtained a molecular weight of 112.9 kDa (Figure 1K), which is consistent with the molecular weight for a 1:1 complex between KBP (71.9 kDa) and His-KIF1A-MD (41 kDa).

Next, we aimed to identify a mechanism that could regulate the KBP-kinesin interaction. Because phosphorylation is an important mechanism to regulate motor function [19], we tested

(C–E) Immunoprecipitations using GFP-trap magnetic beads from extracts of HEK293 cells transfected with the indicated constructs. Blots are probed for GFP and for endogenous KBP. The lower bands in the KIF-MDC-GFP lanes are most likely due to protein degradation.

(F and G) Immunoprecipitations performed as in (C)–(E) comparing C-terminal stalk and tail regions (tail) and MDC (F) and single motor domain (MD) and MDC (G) of the indicated constructs.

(H) Immunoprecipitation performed as in (C)–(E) and pre-treated for 3 hr with either 100 nM okadaic acid (OA) or 1 μM staurosporine (St) and probed for endogenous KBP.

(I) Dephosphorylation assay using recombinant lambda protein phosphatase (λ) and extracts of HEK293 cells transfected with KIF1A-MDC and pre-treated for 3 hr with either 100 nM OA or 1 μM St. PI, protease inhibitor cocktail.

(J) Coomassie-blue-stained SDS-PAGE of purified KBP (lane 1), KBP with His-KIF1A- MD (lane 2), and KBP with His-KIF21B-MD (lane 3) after immobilized metal-affinity chromatography.

(K) Analysis of the molar mass of purified KBP (red line; 69.7 kDa) and co-purified KBP/His-KIF1A-MD complex (black line; 112.9 kDa) by size-exclusion chromatography coupled to multiangle light scattering (SEC-MALS).

(L and M) Circular dichroism (CD) spectrum (L) and thermal unfolding profile (M) of KBP recorded by CD at 222 nm.

See also Figure S1.

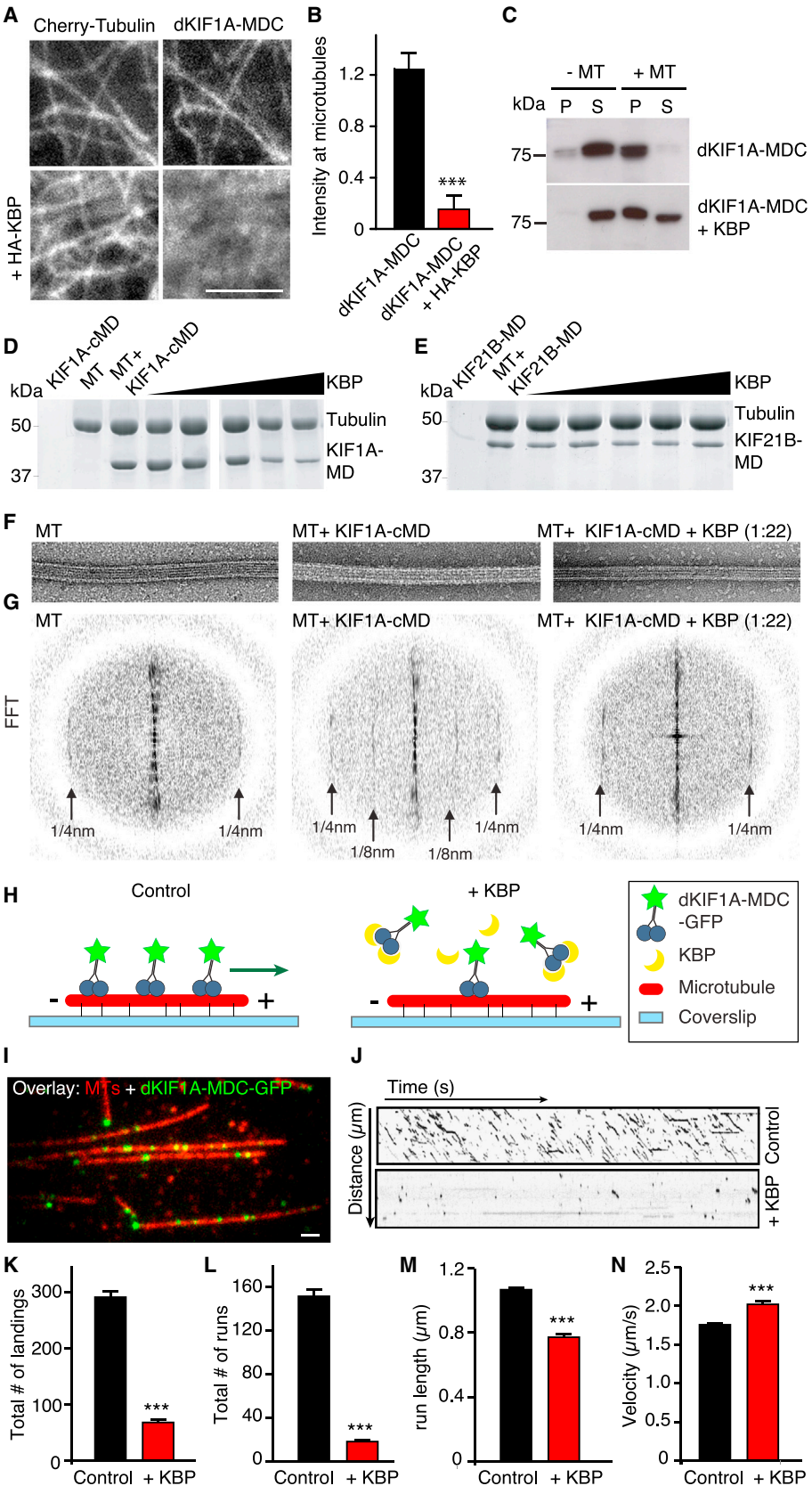

(legend on next page)

whether binding between kinesin and KBP is regulated by phosphorylation. HEK293 cells expressing a panel of KBP-associated KIFs were treated with the phosphatase inhibitor okadaic acid to induce hyperphosphorylation or with the protein kinases inhibitor staurosporine to induce protein dephosporylation (Figure 1H). In addition, recombinant lambda protein phosphatase was added to staurosporin samples to remove additional phosphate groups (Figure 1I). Whereas the treatments did not change the expression of KBP, they reduced the binding of KBP to some kinesins, particularly KIF1A (Figures 1H and 1I). Together, these data demonstrate that KBP binds specifically to the motor domain of a defined subset of kinesin motor proteins and that phosphorylation increases the binding between KBP and some kinesins.

KBP Inhibits KIF1A Motility by Preventing the Association with Microtubules

Because KBP binds specifically to the motor domain of KIF1A, we reasoned that KBP might interfere with the ability of the kinesin to bind to MTs. To test this, we imaged the localization of dimeric GFP-tagged KIF1A (dKIF1A-MDC), generated by fusing the kinesin-1 coiled-coil stalk to the monomeric KIF1A motor domain [20], on mCherry-α-tubulin-labeled MTs in COS-7 cells by total internal reflection fluorescence (TIRF) microscopy. Co-expression of HA-KBP decreased the KIF1A intensity along MTs by ~80% (Figures 2A and 2B). In line with these findings, we observed a strong effect of KBP on the association of dKIF1A-MDC with MTs using MT pelleting assays. dKIF1A-MDC-GFP expressed in HEK293 cells robustly bound to Taxol-stabilized MTs in the absence of KBP, whereas addition of purified $_{KBP}$ strongly decreased MT-KIF association as evidenced by an increased dKIF1A-MDC-GFP fraction observed in the supernatant after centrifugation (Figure 2C). These results were confirmed using recombinant purified proteins: increasing the concentration of KBP reduced the amounts of KIF1A-cMD recovered in the pellet fraction (Figure 2D). In contrast, addition of purified KBP did not affect the MT association of KIF21B-MD (Figure 2E), a kinesin that was not found to interact with KBP (Figure 1D). Micrographs of these pellet fractions verify that MTs are decorated with KIF1A-cMD, as can be observed as small white puncta along the MT, whereas in presence of KBP, they are not (Figure 2F). This observation can be visualized by calculating the fast Fourier transforms (FFTs) of MT segments, which amplifies repetitive patterns. Consistently, MTs alone show a 4 nm periodicity [21] and MTs mixed with KIF1A-cMD a 4 nm and 8 nm periodicity, and, as expected, addition of KBP resulted in loss of the 8 nm periodicity (Figure 2G). These findings suggest that KBP reduces binding of KIF1A-cMD to MTs. Although KBP was previously suggested to associate with the MT cytoskeleton [16, 17], we did not observe a direct interact of KBP with MTs in pelleting assays (Figure S1E). Together, these data demonstrate that KBP prevents binding of KIF1A to MTs.

Because the biochemical experiments showed that KBP inhibits the association of KIF1A with MTs, we next examine the effect of KBP on KIF1A movement along MTs using an in vitro single-molecule motility assay [22]. To visualize the motility of individual KIF1A motors, we added extracts of HEK293 cells expressing GFP-tagged, dimeric KIF1A (dKIF1A-MDC) to surface-immobilized MTs (Figure 2H). Single-KIF1A motors could be observed as distinct fluorescent spots moving unidirectionally along MTs (Figure 2I; Movie S1), and their binding and motility were analyzed using kymographs. Consistent with our MT binding and electron microscopy data (Figures 2A–2G), we observed a strong reduction in the amount of KIF1A motors associating with MTs after addition of purified KBP (Figure 2J). In the presence of KBP, the number of single KIF1A motors that associated with surface-immobilized MTs was reduced by ~75% compared to control (Figure 2K). An even greater reduction of ~85% was observed for the amount of KIF1A motors that were able to move along MTs after addition of KBP (Figure 2L). The few remaining motile particles showed a considerably shorter run length compared to control (Figure 2M) and showed only modest increase in the velocity (Figure 2N). Together, these findings show that KBP inhibits kinesin activity by preventing the association of the kinesin with MTs.

KBP Inhibits Kinesin-Based Cargo Motility in Living Cells

As KBP affects the motility of kinesin along MTs, we hypothesized that KBP might control kinesin-mediated cargo transport. To test this idea, we made use of our previously developed cargo-trafficking assay where FRB-FKBP heterodimerization triggers the coupling of a motor protein of interest to an artificial cargo (in this case, peroxisomes) after addition of the rapamycin analog AP21967 (rapalog; Figure 3A) [23, 24]. In COS-7 cells co-transfected with PEX-RFP-FKBP and KIF-MDC-FRB constructs,

Figure 2. KBP Impairs KIF1A Motility and Its Association with Microtubules

(A) Representative images of cortical areas of COS-7 cells co-expressing mCherry-α-tubulin and GFP-tagged N-terminal fragment of dimeric KIF1A (dKIF1A-MDC-GFP) with and without HA-KBP.

(B) Quantification of dKIF1A-MDC-GFP labeling intensity on MTs with or without co-expression of HA-KBP.

(C) HEK293 cell extracts expressing dKIF1A-MDC-GFP were incubated with (+MT) or without (−MT) Taxol-stabilized MTs and with or without 1 μg/μl purified KBP. The MTs were pelleted, and the supernatant (S) and pellet (P) were analyzed by immunoblotting.

(D and E) SDS-PAGE gels stained with Coomassie blue showing pellets from MT pelleting assays. First lanes represent the control samples: 2.8 μM dKIF1A-MDC (D) or 2.5 μM KIF21B-MD (E; negative control), 3 μM MTs, and MTs mixed with kinesin-MD. Remaining lanes show MTs and kinesin-MD at constant concentration incubated with increasing concentrations of KBP (1.6, 8, 16, 32, and 64 μM KBP).

(F) Electron micrographs of negatively stained pellets from MT pelleting assays showing MTs (MT; smooth lattices); MTs decorated with KIF1A-cMD (MT + KIF1A-cMD; rough lattices); and MTs, KIF1A-cMD, and 22-fold molar excess of KBP (MT + KIF1A-cMD + KBP; smooth lattices).

(G) Fast Fourier transforms (FFTs) calculated from the indicated electron micrograph areas.

(H) Schematic representation of the single-molecule motility assay of dKIF1A-GFP on surface-immobilized MTs without (left) or with KBP (right).

(I) Representative image of dKIF1A-MDC-GFP (green) moving along surface-immobilized MTs (red) in the kinesin-MT motility assay.

(J) Representative kymographs of single dKIF1A-MDC-GFP kinesin movements on a single MT with or without KBP.

(K–N) Quantification of the average total number of kinesins that associate with MTs (landings; K) and the number of processive kinesins along a single MT (L), run length (M), and run velocity (N).

The scale bars represent 3 μm (A) and 100 nm (F); mean values ± SEM; ***$p < 0.001$.

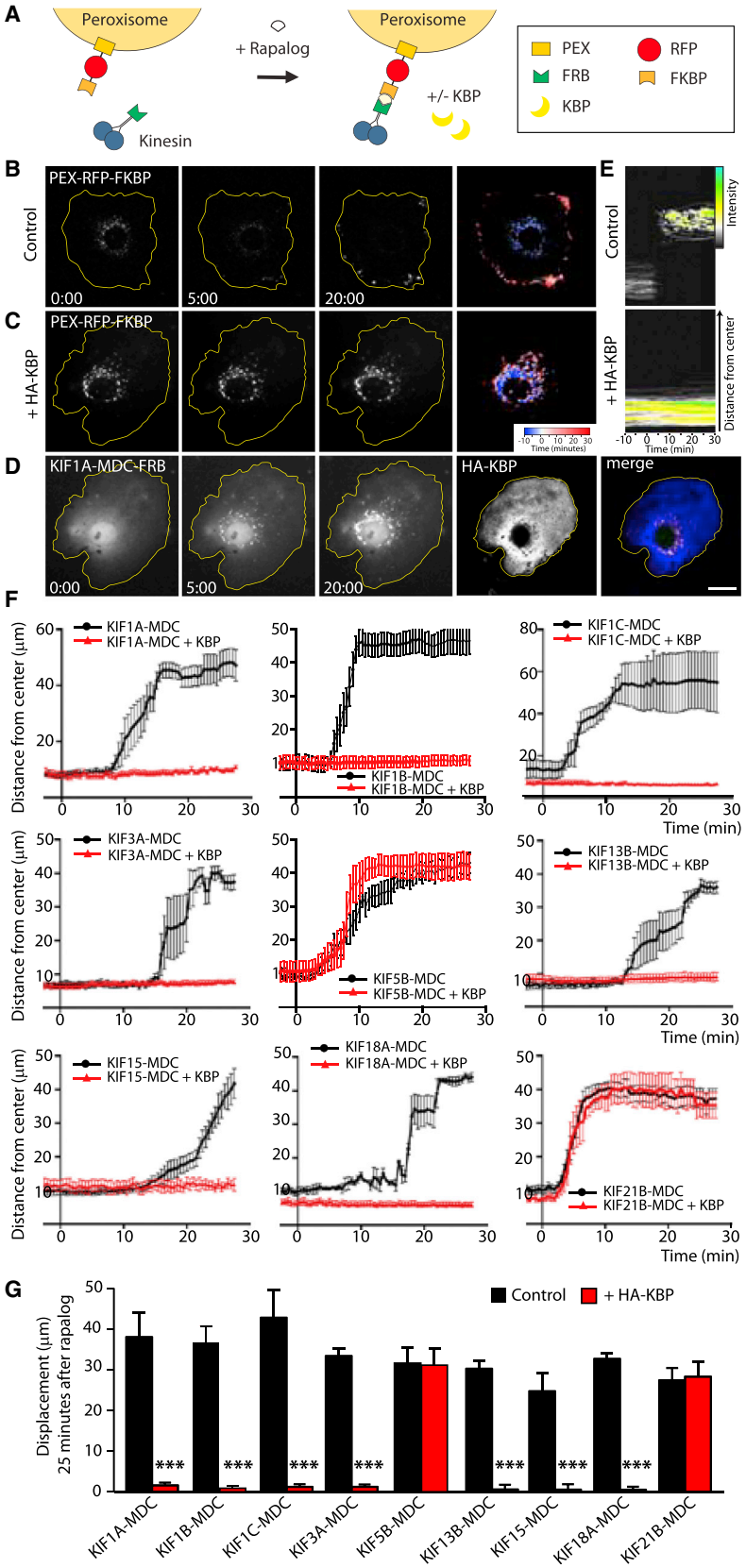

Figure 3. KBP Inhibits Kinesin-Induced Peroxisome Transport

(A) Schematic overview of the inducible cargo-trafficking assay using the FRB-rapalog-FKBP heterodimerization system coupled to peroxisomes.

(B–D) Peroxisome motility in cells visualized by PEX-mRFP-FKBP upon recruitment of KIF1A-MDC-FRB without (B) and with (C) HA-KBP. HA-KBP is detected after fixation by immunofluorescent staining (D). Radial kymograph of recordings acquired with 10 s intervals are shown. The scale bar represents 10 μm.

(E) Overlay of sequential binarized images from the recording in (B) and (C).

(F) Graph showing peroxisome distribution in COS-7 cells over time upon recruitment of the indicated kinesin constructs before and after addition of rapalog with (black lines) and without (red lines) HA-KBP.

(G) The graph shows peroxisome displacement with and without HA-KBP 25 min after rapalog addition. Mean values ± SEM; ***$p < 0.001$.

See also Figure S3.

most peroxisomes displayed a perinuclear localization before rapalog addition (0 min; Figure 3B). Treating these cells with rapalog revealed a robust accumulation over time of peroxisomes at the cell periphery, near MT plus ends (Figures 3B and 3E). Co-expressing peroxisome targeting and kinesin motor constructs together with full-length HA-KBP prevents the directional translocation of peroxisomes to the cell periphery by all KBP-interacting kinesins, but, as expected, not by KIF5B or KIF21B (Figures 3C–3G, S2A, and S2B; Movies S2 and S3). These findings suggest that KBP inhibits cargo transport driven by a specific subset of kinesin motors. Importantly, expression of HA-KBP in COS-7 cells does not interfere with the heterodimerization system itself (Figures 3C, 3D, and S2E). Consistent with the pull-down experiments (Figures 1B and S1C), the co-expression of truncated fragments of KBP was not able to inhibit the translocation of KIF1A (Figures S2C and S2D). All these findings were further confirmed using fixed HeLa cells treated with rapalog for different time intervals (Figures S2F–S2H). Collectively, these findings indicate that KBP inhibits kinesin activity by preventing the association of the kinesin with MTs.

KBP Controls Microtubule Dynamics in Neurons

KBP has previously been reported to be required for axonal development in zebrafish [18]. Therefore, we investigated the role of KBP in axonal outgrowth using primary cultured hippocampal neurons. We transfected neurons at DIV0 with HA-KBP for 4 days and found that overexpression of KBP resulted in reduced axon length (Figures S3A and S3B). In contrast, depletion of KIF1A using small hairpin RNA (shRNA) did not result in a similar decrease in axon outgrowth, consistent with the absence of clear morphological phenotypes in KIF1A-deficient neurons [25]. Either increasing or decreasing KBP levels results in a high number of neurons with Golgi fragmentation, similar to the KIF1C knockdown phenotype (Figures S3C and S3D). Interestingly, electron microscopy analysis of KBP zebrafish mutants revealed MT defects [18], although the exact mechanism has remained unresolved. Therefore, we tested the effect of KBP on MT dynamics in neurons by expressing GFP-MACF43 (GFP-MT+TIP) to specifically label growing MT plus ends using live-cell imaging [26] (Figure 4A). Expression of HA-KBP greatly affects several parameters of MT dynamics, such as the MT growth length, growth rate, and catastrophe frequency compared to control cells (Figures 4B–4D). As KBP functions as a kinesin inhibitor, we reasoned that reduced levels of a MT-dynamics-regulating kinesin should display similar effects on MT dynamics as KBP overexpression. From the KBP-interacting kinesins, only KIF18A, a member of the kinesin-8 family, is known to function as a MT-depolymerizing kinesin during mitotic chromosome positioning [27, 28]. Depletion of KIF18A affects MT dynamics in post-mitotic neurons, similar to KBP overexpression (Figures 4A–4D) which could be rescued by co-expression of full-length KIF18A (Figures 4A–4D). We observed an increase in catastrophe frequency in KIF18A knockdown neurons, which is unexpected for a MT-depolymerizing kinesin, but this effect has been reported before for kinesin-8 family members [29]. The MT growth rate was increased in KIF18A depleted (Figure 4C), which is in line with a role of KIF18A in promoting MT pausing [27, 28]. As expected, KIF1A depletion had no effect on catastrophe frequency or growth length (Figures 4A–4D). Because various depolymerizing kinesins have been implicated in axon outgrowth [30], we tested the effect of KIF18A depletion and observed a decrease in axon length, comparable to KBP overexpression (Figures S3A and S3B). Together, these data suggest that KBP controls MT dynamics by controlling the activity of MT-regulating kinesins.

KBP Controls KIF1A-Mediated Synaptic Vesicle Distributions

As we found that KBP controls kinesin-mediated cargo trafficking in cells, and as KBP mutant zebrafish show aberrant organelle accumulations in the axon [18], we next determined the role of KBP in axonal cargo transport. HA-KBP localizes to the cytoplasm with a variety of distinct puncta scattered throughout the cell body, axon, and dendrites, which do not specifically coincide with neuronal cargoes, such as Rab3-positive synaptic vesicle precursors, autophagosome adaptor LC3, or mitochondria (Figure 4E). Because KBP interacts with KIF1A (Figures 1A and 1D), which mediates axonal transport of Rab3-positive synaptic vesicle precursors [25, 31, 32], we studied the effect of KBP on KIF1A localization. We transfected DIV4-cultured hippocampal neurons with myc-KIF1A together with KBP overexpression or knockdown constructs for 4 days. Changing the level of KBP resulted in a marked change in KIF1A localization: knockdown of KBP resulted in an increase of KIF1A in the distal tips of neurites, whereas HA-KBP expression leads to a KIF1A accumulation in the proximal axon (Figures 4F and 4G). As expected, the KIF1A-mediated cargo Rab3 followed a comparable distribution upon KBP depletion and overexpression (Figures 4H–4J). Control hippocampal neurons showed GFP-Rab3-labeled synaptic vesicles in the cell body and in proximal and distal axons, whereas KBP-depleted cells showed a strong increase in Rab3 intensity in the distal axon (Figures 4H–4J), similar to the overexpression of HA-KIF1A and HA-KIF1Bβ (Figures 4H–4J), another KBP-associated kinesin implicated in Rab3 transport. In contrast, overexpression of KBP resulted in a marked decrease in Rab3 intensity in the distal axons (Figures 4H–4J) and increased Rab3 intensity in the cell body (Figure 4K), similar to KIF1A depletion (Figures 4F and 4G), which is in line with previous findings on synaptic vesicle distributions in KIF1A-deficient mice [25]. Consistently, increased or decreased levels of KBP leads to an increase or decrease in the number of neurons displaying Rab3 accumulations in the cell body, respectively (Figure 4L). Simultaneous depletion of KIF1A or KIF1B was able to rescue the effect of HA-KBP on Rab3 accumulation in the cell body (Figure 4L). These findings show that KBP is required for the normal distribution of synaptic vesicle precursors in hippocampal neurons and indicate that KBP prevents the transport of Rab3 vesicles by inhibiting kinesin motor activity.

Next, we studied the role of KBP in controlling Rab3 distributions in *C. elegans*, as an in vivo model system. In contrast to mammals, *C. elegans* does not have a gene encoding for KBP. We therefore generated transgenic worms expressing GFP-tagged human KBP in PVD sensory neurons (Figure 4M) and examined the axonal targeting of the presynaptic marker RAB-3, which depends on UNC-104/KIF1A [33]. To verify that KBP is able to bind UNC-104, we performed immunoprecipitation experiments in HEK293 cells using a construct containing

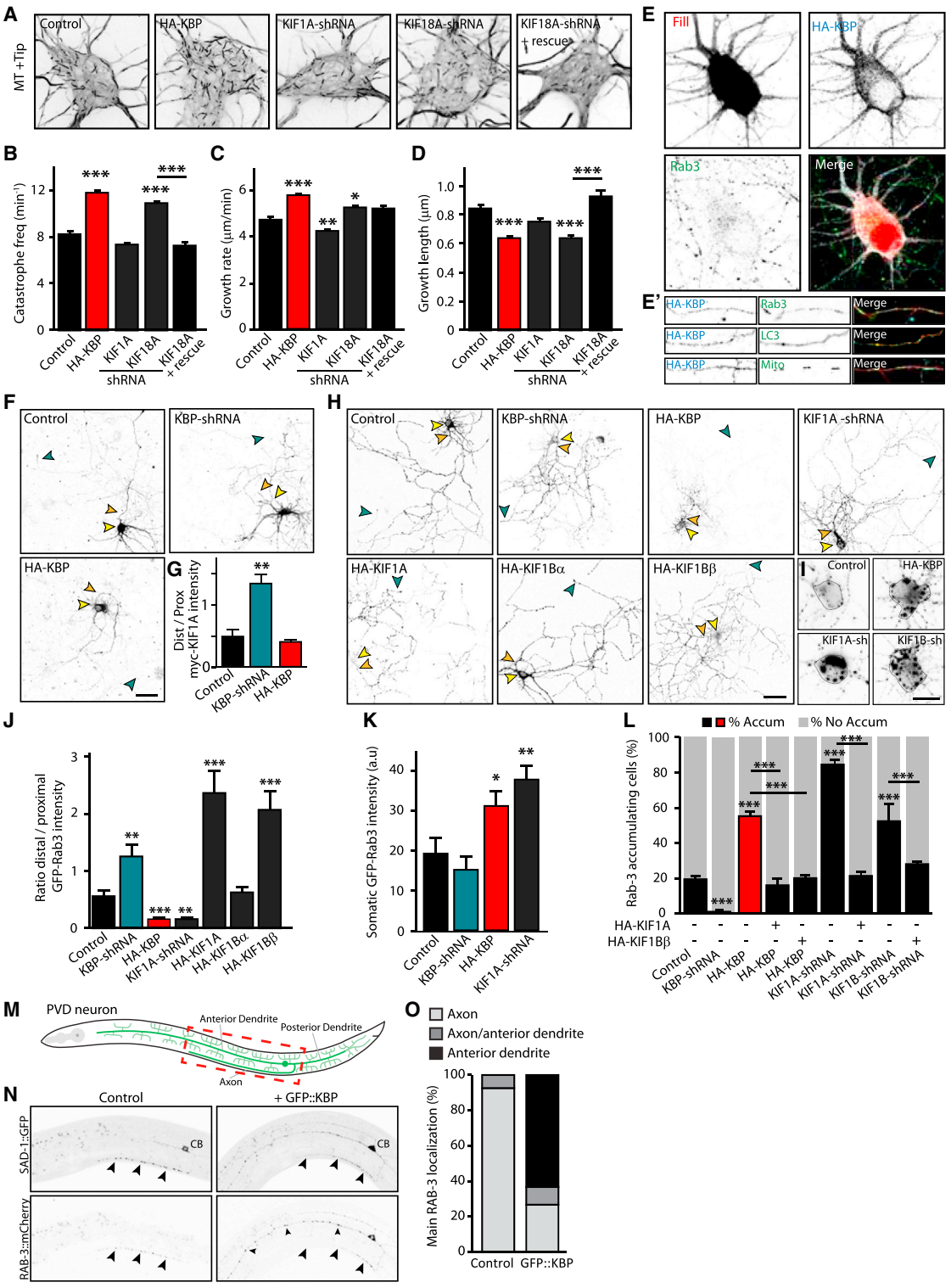

Figure 4. KBP Controls Microtubule Dynamics and Synaptic Vesicle Distributions

(A) Representative images of maximum intensity projections of GFP-MT+TIP in the cell body of neurons cotransfected with the indicated constructs (DIV4+4).

(B–D) Quantification of the average catastrophe frequency (B), growth rate (C), and growth length (D) of MT plus ends marked by GFP-MT+TIP.

(E) Representative images of neurons (DIV4+4) co-transfected with HA-KBP and RFP or GFP (fill) stained for HA and endogenous Rab3 or co-transfected with RFP-LC3 or Mito-dsRed.

(legend continued on next page)

the motor domain and the first coiled coil (MDC) of UNC-104 (Figure S1F). In wild-type animals, presynaptic specializations are largely restricted to the axon in the ventral nerve cord of the PVD [33]. Expression of GFP-KBP alters the distributions of RAB-3-mCherry, resulting in mislocalization of the synaptic vesicles from the axon to the cell body and in the anterior dendrite (Figures 4N and 4O). These observations suggest that KBP alters the UNC-104/KIF1A-mediated distribution of synaptic vesicles. Collectively, these results demonstrate that KBP inhibits KIF1A-dependent synaptic vesicle distribution.

KBP Regulates Transport of Axonal Cargoes

Because KBP regulates the distribution of Rab3 vesicles in neurons, we next determined the effect of KBP on the motility of synaptic vesicles. First, we transfected DIV4-cultured hippocampal neurons with GFP-Rab3 for 4 days and followed their movements in axons using live-cell microscopy (Figure 5A; Movie S4). Co-expression of HA-KBP resulted in a strong decrease of motile Rab3 vesicles and in an increase of static vesicles in axons, whereas KBP depletion showed the opposite effect (Figures 5B and 5C). Using kymographs, we analyzed the velocities of moving Rab3 vesicles and observed an average velocity of 1.21 ± 0.05 μm/s for anterograde moving vesicles in control neurons (Figures 5D and S4A), which is consistent with reported velocities [34–36]. Compared to control, we observed a significant decrease in anterograde Rab3 vesicle speed after co-expression of HA-KBP to 0.81 ± 0.05 μm/s (Figures 5D and S4A). As expected, depletion of KIF1A showed the same effect on Rab3 vesicle motility as KBP overexpression (Figures 5D and S4A). In contrast, Rab3 vesicles moved faster toward the distal axon upon depletion of KBP with an average velocity of 1.76 ± 0.11 μm/s (Figures 5D and S4A), which is comparable with the velocity of KIF1A in the in vitro motility assay (Figure 2N). Although less pronounced, a similar effect of KBP overexpression and knockdown was observed for Rab3 vesicles moving in a retrograde direction (Figures 5C and S4B). The observed Rab3-trafficking defects in KBP overexpression and knockdown neurons was not due to altered MT dynamics because we found no alterations in the axonal MT polarity (Figures S4C and S4D) or defects in Rab3 motility upon changes in KIF18 activity levels (Figures S4E and S4F). KIF5 and dynein, motors that do not bind KBP (Figures 1B–1D), are the main motors that drive both axonal mitochondrial and autophagosome transport [37–39]. In contrast, overexpression of KBP does not modulate the velocity and number of anterograde moving mitochondria (Figures 5F, 5G, and 5I) or the velocity of anterograde autophagosome transport (Figures 5J and 5K), which is consistent with their KIF5-mediated transport. However, KBP depletion affects the velocity and number of retrograde moving mitochondria (Figure 5I) and the number of retrograde moving autophagosomes (Figure 5M), suggesting that some KBP-associated kinesin motors play an additional role in coordinate bidirectional axonal transport. These findings support the idea that motor teams of opposite polarity are required for driving efficient cargo transport [40]. Collectively, our findings indicate that KBP regulates the trafficking of axonal cargoes by controlling kinesin activity.

DISCUSSION

KBP Controls Microtubule Dynamics and Cargo Transport

It has been shown that KBP is required for axonal outgrowth and maintenance in zebrafish *kbp*-null mutants [18]; axons show reduced growth during development and undergo degeneration at later stages. Moreover, electron microscopy analysis revealed aberrant cargo accumulations in the axon and an abnormal distribution of synaptic vesicles [18]. Our findings in KBP-depleted hippocampal neurons are consistent with the reported observations in zebrafish *kbp* mutants, as we observed impaired neuronal development and abnormal localization of synaptic vesicle precursors. It has previously been suggested that KBP is a MT-associated protein whose main role is to regulate MT organization in neurons [16, 17]. It has also been proposed that the abnormal cargo localization observed in zebrafish mutants might occur as a secondary effect of the altered MT cytoskeleton [18]. In contrast to these conclusions, we found that KBP does not directly bind to MTs but can alter MT dynamics by inhibiting the activity of MT-depolymerizing kinesins, such as KIF18A. Our results suggest that KBP influences kinesins that are required for both MT cytoskeleton organization and neuronal cargo transport mechanisms. Therefore, we propose that the primary function of KBP is to regulate a subset of kinesins required for distinct neuronal kinesin-dependent processes.

KBP-Controlled Kinesin Motor Activity Is Required for Distinct Neuron Developmental Processes

In this study, we have mainly used KIF1A as a representative motor protein to investigate the KBP-kinesin interaction in biochemical, biophysical, and cellular experiments. Our data suggest that KBP functions as a regulator of KIF1A motor activity and controls KIF1A-mediated synaptic vesicle precursor (Rab3) transport in hippocampal neurons. We found that KBP not only interacts with KIF1A but also with several other kinesin family members. Defects in multiple KBP-controlled kinesin pathways could together account for the axonal outgrowth and synaptic vesicle phenotypes observed in KBP-deficient neurons and in KBP mutant zebrafish [18]. Because KIF1A-deficient neurons do not show clear morphological alterations during development [25],

(F and G) Representative images (F) and quantification (G) of myc-KIF1A localization in neurons (DIV4+4) co-transfected with the indicated constructs. Arrows indicate the soma (yellow), proximal axon (orange), and distal axon (green).

(H–L) Representative images (H and I) and quantifications (J, K, and L) of GFP-Rab3 expression neurons (H) and in the cell body (I) of neurons (DIV4+4) transfected with the indicated constructs and GFP-Rab3.

(M) Schematic representation of the *C. elegans* PVD neuron.

(N) Representative images of *C. elegans* PVD neuron, showing localization of synaptic vesicles marked by RAB-3-mCherry and SAD-1-GFP in worms with or without GFP-KBP. CB, cell body.

(O) Quantification of the percentage of RAB-3 vesicle localization in control worms or worms overexpressing KBP.

Scale bars represent 5 μm (E′ and I), 10 μm (A, E, F, and H), and 20 μm (N); mean values ± SEM; ***$p < 0.001$; **$p < 0.01$; *$p < 0.05$. See also Figures S1 and S3.

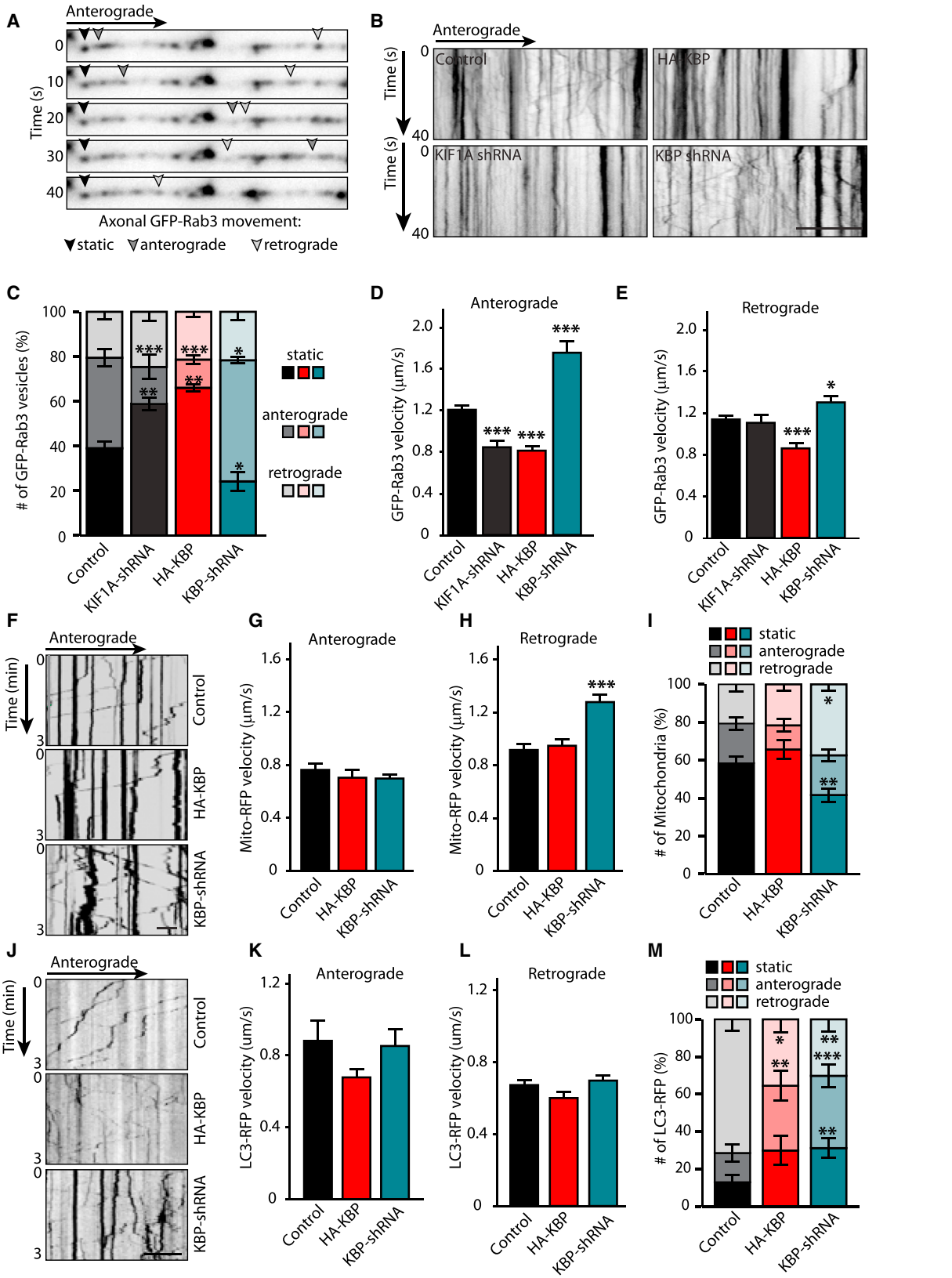

(legend on next page)

our observed axonal defects could be attributed to the impairment processes mediated by other KBP-controlled kinesins. For example, KIF13B is known to be involved in neurite extension via the transport of PIP3-containing lipid vesicles to the axon tips [41–44]. In addition, we demonstrated that alterations in MT dynamics and mediated by KIF18A [27, 28] may, at least partly, account for the developmental defects. Interestingly, in this respect are the findings that homozygous nonsense mutations in the gene encoding KBP were linked to GOSHS [10–12]. Future studies should address whether misregulation of a specific set of KBP-controlled kinesins contribute to the neuropathological defects observed in GOSHS patients.

KBP Provides a Novel Mechanism for Controlling Kinesin Activity

Using single-molecule in vitro assays, we found that KBP inhibits kinesin motility by blocking the association of KIF1A with MTs. However, unlike autoinhibition, the inhibitory function of KBP is not restricted to cytoplasmic motors but can also block cargo-attached kinesin movement. These observations imply that KBP binding to kinesins may be able to directly control the bidirectional movement of axonal cargos that are transported by opposing motors. Moreover, as seen for mitochondria and autophagosome trafficking, the repertoire of KBP-controlled kinesins and other motors bound to transport vesicles will dictate the exact transport parameters and allow precise spatial and temporal regulation to ensure proper motility and delivery of specific cargoes.

The simplest model for how KBP controls kinesin function is the one in which KBP binding to the motor domain inhibits kinesin activity and where release of KBP activates kinesin motors to allow kinesin function. We found that phosphorylation enhances the binding between KBP and KIF1A. Investigating whether local kinase signaling affects the activity of KBP and whether other post-translational modifications influence kinesin-KBP complex formation will be important topics for future studies. Because we found that KBP interacts with a subset of partially unrelated motor proteins, it remains an intriguing question why KBP preferentially binds and inhibits the motility of this specific set because we could not identify an obvious consensus sequence in their motor domains. Solving the high-resolution structure of the KBP-kinesin complex will be necessary to resolve this issue.

EXPERIMENTAL PROCEDURES

Animals and Ethics Statement

All animal experiments were performed in compliance with the guidelines for the welfare of experimental animals issued by the federal government of the Netherlands. All animal experiments were approved by the Animal Ethical Review Committee (DEC) of the Erasmus Medical Center and Utrecht University.

Antibodies and Reagents

Two independent anti-KBP antibodies were generated by immunizing rabbits with a short peptide encompassing aa 24–38 of mouse KBP (Eurogentec) and glutathione S-transferase (GST)-KBP (aa 1–292) fusion proteins. Details of KBP antisera and other antibodies and reagents are in the Supplemental Experimental Procedures.

DNA and shRNA Constructs

The KBP expression constructs were generated by a PCR-based strategy using the human KBP cDNA (KIAA1279; IMAGE clone 4550085). The KBP-shRNA sequence (5′-TATCATAGTAAGCATGTGCTT) targeting rat KBP mRNA (NP_001026797) was based on the effective human KBP no. 1 siRNA sequence and inserted into a pSuper vector. See the Supplemental Experimental Procedures.

Protein Purification and Biophysical Characterization

KBP was expressed in Rosetta2 cells, lysed, and purified by immobilized metal-affinity chromatography (IMAC) followed by size-exclusion chromatography. MALS was performed using an S-200 analytical size-exclusion chromatography column connected in line to a mini-DAWN TREOS light-scattering and Optilab T-rEX refractive index detectors. For details, see the Supplemental Experimental Procedures.

In Vitro Kinesin Motility Assay

MTs labeled with rhodamine-conjugated tubulin were stabilized and attached to a glass coverslip. Dimeric GFP-tagged KIF1A was expressed in HEK293 cells, and cell lysates were added, in the presence of ATP, to the stabilized MTs and incubated with or without purified KBP. For details, see the Supplemental Experimental Procedures.

Data Representation and Statistics

In all bar graphs, data are presented as mean values ± SEM. Data samples were tested for normal distribution. The independent t test or the non-parametric Mann-Whitney U was used for pairwise comparisons. For multiple comparisons, the Kruskal-Wallis test with pairwise comparisons was used. n indicates the number of independent experiments.

SUPPLEMENTAL INFORMATION

Supplemental Information includes Supplemental Experimental Procedures, four figures, and four movies and can be found with this article online at http://dx.doi.org/10.1016/j.cub.2016.01.048.

AUTHOR CONTRIBUTIONS

J.T.K. performed cellular experiments and wrote the manuscript; S.B., N.O., and M. Hilbert performed biophysical, biochemical, and electron microscope experiments; M.v.S. performed pull-down experiments and rapalog assay in fixed cells; J.L. performed rapalog assay in living cells; C.P.F. performed morphology analysis; L.C.K. and M.M. conducted biochemistry and in vitro experiments; and M. Harterink performed *C. elegans* experiments. N.K. and

Figure 5. KBP Controls Axonal Vesicle Trafficking in Living Neurons

(A) Live-cell imaging was used to visualize GFP-Rab3 vesicle movement along the axon in DIV4+4 neurons. Static Rab3 vesicles (black arrowhead) and moving vesicles in the anterograde (dark gray arrowheads) or retrograde (light gray arrowheads) direction are indicated.

(B–E) Representative kymographs (B) and quantification (C–E) showing motility of GFP-Rab3 in axons co-transfected with the indicated constructs as described in (A).

(F–I) Representative kymograph (F) and quantification (G–I) showing axonal mitochondria movement in neurons transfected with Mito-dsRed and indicated constructs in DIV4+4 neurons.

(J–M) Representative kymograph (J) and quantification (K–M) showing axonal autophagosome movement in neurons transfected with LC3-RFP and indicated constructs in DIV4+4 neurons.

Scale bars represent 10 μm (F and J); mean values ± SEM; ***$p < 0.001$; **$p < 0.01$; *$p < 0.05$. See also Figure S4.

P.S.W. provided technical assistance; E.d.G., L.C.K., and A.A. gave advice throughout the project; and M.O.S. and C.C.H. supervised the research, coordinated the study, and wrote the manuscript with the input from the authors.

ACKNOWLEDGMENTS

We thank Jeroen Demmers for help with mass spectrometry analyses. This work was supported by the Erasmus Medical Center (EMC fellowship to L.C.K.), the Netherlands Organization for Scientific Research (NWO-VENI to L.C.K. and M. Harterink and NWO-ALW-VICI to A.A. and C.C.H.), the Netherlands Organization for Health Research and Development (ZonMW-TOP to C.C.H.), the Marie-Curie Intra-European Fellowship (to M.M.), the European Science Foundation (EURYI to C.C.H.), and by a grant from the Swiss National Science Foundation (310030B_138659 to M.O.S.).

Received: November 24, 2015
Revised: December 31, 2015
Accepted: January 20, 2016
Published: March 3, 2016

REFERENCES

1. Hirokawa, N., Niwa, S., and Tanaka, Y. (2010). Molecular motors in neurons: transport mechanisms and roles in brain function, development, and disease. Neuron *68*, 610–638.
2. Vale, R.D. (2003). The molecular motor toolbox for intracellular transport. Cell *112*, 467–480.
3. Walczak, C.E., Gayek, S., and Ohi, R. (2013). Microtubule-depolymerizing kinesins. Annu. Rev. Cell Dev. Biol. *29*, 417–441.
4. Janke, C., and Kneussel, M. (2010). Tubulin post-translational modifications: encoding functions on the neuronal microtubule cytoskeleton. Trends Neurosci. *33*, 362–372.
5. Schlager, M.A., and Hoogenraad, C.C. (2009). Basic mechanisms for recognition and transport of synaptic cargos. Mol. Brain *2*, 25.
6. Verhey, K.J., and Hammond, J.W. (2009). Traffic control: regulation of kinesin motors. Nat. Rev. Mol. Cell Biol. *10*, 765–777.
7. Kaan, H.Y., Hackney, D.D., and Kozielski, F. (2011). The structure of the kinesin-1 motor-tail complex reveals the mechanism of autoinhibition. Science *333*, 883–885.
8. Blasius, T.L., Cai, D., Jih, G.T., Toret, C.P., and Verhey, K.J. (2007). Two binding partners cooperate to activate the molecular motor Kinesin-1. J. Cell Biol. *176*, 11–17.
9. Coy, D.L., Hancock, W.O., Wagenbach, M., and Howard, J. (1999). Kinesin's tail domain is an inhibitory regulator of the motor domain. Nat. Cell Biol. *1*, 288–292.
10. Brooks, A.S., Bertoli-Avella, A.M., Burzynski, G.M., Breedveld, G.J., Osinga, J., Boven, L.G., Hurst, J.A., Mancini, G.M., Lequin, M.H., de Coo, R.F., et al. (2005). Homozygous nonsense mutations in KIAA1279 are associated with malformations of the central and enteric nervous systems. Am. J. Hum. Genet. *77*, 120–126.
11. Dafsari, H.S., Byrne, S., Lin, J.P., Pitt, M., Jongbloed, J.D., Flinter, F., and Jungbluth, H. (2015). Goldberg-Shprintzen megacolon syndrome with associated sensory motor axonal neuropathy. Am. J. Med. Genet. A. *167*, 1300–1304.
12. Valence, S., Poirier, K., Lebrun, N., Saillour, Y., Sonigo, P., Bessières, B., Attié-Bitach, T., Benachi, A., Masson, C., Encha-Razavi, F., et al. (2013). Homozygous truncating mutation of the KBP gene, encoding a KIF1B-binding protein, in a familial case of fetal polymicrogyria. Neurogenetics *14*, 215–224.
13. Wozniak, M.J., Melzer, M., Dorner, C., Haring, H.U., and Lammers, R. (2005). The novel protein KBP regulates mitochondria localization by interaction with a kinesin-like protein. BMC Cell Biol. *6*, 35.
14. Lehti, M.S., Kotaja, N., and Sironen, A. (2013). KIF3A is essential for sperm tail formation and manchette function. Mol. Cell. Endocrinol. *377*, 44–55.
15. Tanaka, K., Sugiura, Y., Ichishita, R., Mihara, K., and Oka, T. (2011). KLP6: a newly identified kinesin that regulates the morphology and transport of mitochondria in neuronal cells. J. Cell Sci. *124*, 2457–2465.
16. Alves, M.M., Burzynski, G., Delalande, J.M., Osinga, J., van der Goot, A., Dolga, A.M., de Graaff, E., Brooks, A.S., Metzger, M., Eisel, U.L., et al. (2010). KBP interacts with SCG10, linking Goldberg-Shprintzen syndrome to microtubule dynamics and neuronal differentiation. Hum. Mol. Genet. *19*, 3642–3651.
17. Drévillon, L., Megarbane, A., Demeer, B., Matar, C., Benit, P., Briand-Suleau, A., Bodereau, V., Ghoumid, J., Nasser, M., Decrouy, X., et al. (2013). KBP-cytoskeleton interactions underlie developmental anomalies in Goldberg-Shprintzen syndrome. Hum. Mol. Genet. *22*, 2387–2399.
18. Lyons, D.A., Naylor, S.G., Mercurio, S., Dominguez, C., and Talbot, W.S. (2008). KBP is essential for axonal structure, outgrowth and maintenance in zebrafish, providing insight into the cellular basis of Goldberg-Shprintzen syndrome. Development *135*, 599–608.
19. Hirokawa, N., Nitta, R., and Okada, Y. (2009). The mechanisms of kinesin motor motility: lessons from the monomeric motor KIF1A. Nat. Rev. Mol. Cell Biol. *10*, 877–884.
20. Tomishige, M., Klopfenstein, D.R., and Vale, R.D. (2002). Conversion of Unc104/KIF1A kinesin into a processive motor after dimerization. Science *297*, 2263–2267.
21. Harrison, B.C., Marchese-Ragona, S.P., Gilbert, S.P., Cheng, N., Steven, A.C., and Johnson, K.A. (1993). Decoration of the microtubule surface by one kinesin head per tubulin heterodimer. Nature *362*, 73–75.
22. Kapitein, L.C., Peterman, E.J., Kwok, B.H., Kim, J.H., Kapoor, T.M., and Schmidt, C.F. (2005). The bipolar mitotic kinesin Eg5 moves on both microtubules that it crosslinks. Nature *435*, 114–118.
23. Hoogenraad, C.C., Wulf, P., Schiefermeier, N., Stepanova, T., Galjart, N., Small, J.V., Grosveld, F., de Zeeuw, C.I., and Akhmanova, A. (2003). Bicaudal D induces selective dynein-mediated microtubule minus end-directed transport. EMBO J. *22*, 6004–6015.
24. Kapitein, L.C., Schlager, M.A., van der Zwan, W.A., Wulf, P.S., Keijzer, N., and Hoogenraad, C.C. (2010). Probing intracellular motor protein activity using an inducible cargo trafficking assay. Biophys. J. *99*, 2143–2152.
25. Yonekawa, Y., Harada, A., Okada, Y., Funakoshi, T., Kanai, Y., Takei, Y., Terada, S., Noda, T., and Hirokawa, N. (1998). Defect in synaptic vesicle precursor transport and neuronal cell death in KIF1A motor protein-deficient mice. J. Cell Biol. *141*, 431–441.
26. Yau, K.W., van Beuningen, S.F., Cunha-Ferreira, I., Cloin, B.M., van Battum, E.Y., Will, L., Schätzle, P., Tas, R.P., van Krugten, J., Katrukha, E.A., et al. (2014). Microtubule minus-end binding protein CAMSAP2 controls axon specification and dendrite development. Neuron *82*, 1058–1073.
27. Mayr, M.I., Hümmer, S., Bormann, J., Grüner, T., Adio, S., Woehlke, G., and Mayer, T.U. (2007). The human kinesin Kif18A is a motile microtubule depolymerase essential for chromosome congression. Curr. Biol. *17*, 488–498.
28. Stumpff, J., von Dassow, G., Wagenbach, M., Asbury, C., and Wordeman, L. (2008). The kinesin-8 motor Kif18A suppresses kinetochore movements to control mitotic chromosome alignment. Dev. Cell *14*, 252–262.
29. Gardner, M.K., Zanic, M., Gell, C., Bormuth, V., and Howard, J. (2011). Depolymerizing kinesins Kip3 and MCAK shape cellular microtubule architecture by differential control of catastrophe. Cell *147*, 1092–1103.
30. Noda, Y., Niwa, S., Homma, N., Fukuda, H., Imajo-Ohmi, S., and Hirokawa, N. (2012). Phosphatidylinositol 4-phosphate 5-kinase alpha (PIPKα) regulates neuronal microtubule depolymerase kinesin, KIF2A and suppresses elongation of axon branches. Proc. Natl. Acad. Sci. USA *109*, 1725–1730.
31. Hall, D.H., and Hedgecock, E.M. (1991). Kinesin-related gene unc-104 is required for axonal transport of synaptic vesicles in C. elegans. Cell *65*, 837–847.
32. Zhao, C., Takita, J., Tanaka, Y., Setou, M., Nakagawa, T., Takeda, S., Yang, H.W., Terada, S., Nakata, T., Takei, Y., et al. (2001). Charcot-Marie-Tooth

disease type 2A caused by mutation in a microtubule motor KIF1Bbeta. Cell *105*, 587–597.

33. Maniar, T.A., Kaplan, M., Wang, G.J., Shen, K., Wei, L., Shaw, J.E., Koushika, S.P., and Bargmann, C.I. (2012). UNC-33 (CRMP) and ankyrin organize microtubules and localize kinesin to polarize axon-dendrite sorting. Nat. Neurosci. *15*, 48–56.
34. Lee, J.R., Shin, H., Ko, J., Choi, J., Lee, H., and Kim, E. (2003). Characterization of the movement of the kinesin motor KIF1A in living cultured neurons. J. Biol. Chem. *278*, 2624–2629.
35. Mondal, S., Ahlawat, S., Rau, K., Venkataraman, V., and Koushika, S.P. (2011). Imaging in vivo neuronal transport in genetic model organisms using microfluidic devices. Traffic *12*, 372–385.
36. Okada, Y., Yamazaki, H., Sekine-Aizawa, Y., and Hirokawa, N. (1995). The neuron-specific kinesin superfamily protein KIF1A is a unique monomeric motor for anterograde axonal transport of synaptic vesicle precursors. Cell *81*, 769–780.
37. Fu, M.M., Nirschl, J.J., and Holzbaur, E.L. (2014). LC3 binding to the scaffolding protein JIP1 regulates processive dynein-driven transport of autophagosomes. Dev. Cell *29*, 577–590.
38. Hollenbeck, P.J., and Saxton, W.M. (2005). The axonal transport of mitochondria. J. Cell Sci. *118*, 5411–5419.
39. van Spronsen, M., Mikhaylova, M., Lipka, J., Schlager, M.A., van den Heuvel, D.J., Kuijpers, M., Wulf, P.S., Keijzer, N., Demmers, J., Kapitein, L.C., et al. (2013). TRAK/Milton motor-adaptor proteins steer mitochondrial trafficking to axons and dendrites. Neuron *77*, 485–502.
40. Ally, S., Larson, A.G., Barlan, K., Rice, S.E., and Gelfand, V.I. (2009). Opposite-polarity motors activate one another to trigger cargo transport in live cells. J. Cell Biol. *187*, 1071–1082.
41. Horiguchi, K., Hanada, T., Fukui, Y., and Chishti, A.H. (2006). Transport of PIP3 by GAKIN, a kinesin-3 family protein, regulates neuronal cell polarity. J. Cell Biol. *174*, 425–436.
42. Nishimura, T., Kato, K., Yamaguchi, T., Fukata, Y., Ohno, S., and Kaibuchi, K. (2004). Role of the PAR-3-KIF3 complex in the establishment of neuronal polarity. Nat. Cell Biol. *6*, 328–334.
43. Shi, S.H., Cheng, T., Jan, L.Y., and Jan, Y.N. (2004). APC and GSK-3beta are involved in mPar3 targeting to the nascent axon and establishment of neuronal polarity. Curr. Biol. *14*, 2025–2032.
44. Yoshimura, Y., Terabayashi, T., and Miki, H. (2010). Par1b/MARK2 phosphorylates kinesin-like motor protein GAKIN/KIF13B to regulate axon formation. Mol. Cell. Biol. *30*, 2206–2219.